

Bioactivation of the Pulmonary Toxicants Naphthalene and 1-Nitronaphthalene by Rat CYP2F4

R. Michael Baldwin, Michael A. Shultz, and Alan R. Buckpitt

Department of Molecular Biosciences, School of Veterinary Medicine, University of California, Davis, California

Received August 1, 2004; accepted October 26, 2004

ABSTRACT

Naphthalene, a ubiquitous environmental contaminant, produces cytotoxicity in nonciliated bronchiolar epithelial (Clara) cells in mice; rats are refractory to lung cytotoxicity from naphthalene. In contrast, 1-nitronaphthalene is a potent toxicant in both species. Naphthalene is metabolized by CYP2F to a 1,2-epoxide, the first and obligate step in events leading to cytotoxicity. 1-Nitronaphthalene is metabolized to both the 5,6- and the 7,8-epoxides with the 7,8-epoxide predominating in lung. Previous studies have demonstrated recombinant CYP2F2 (mouse) to efficiently metabolize both naphthalene and 1-nitronaphthalene. To better understand the mechanism for the unique toxicity profiles for both compounds, a CYP2F ortholog (CYP2F4) was isolated from rat lung and expressed using a baculovirus system. Recombinant CYP2F4 efficiently generates 1*R*,2*S*-naphthalene oxide ($K_m = 3 \mu\text{M}$, $V_{\max} = 107 \text{ min}^{-1}$) and the 5,6- and 7,8-epoxides of 1-nitronaphthalene ($K_m = 18$

μM , $V_{\max} = 25 \text{ min}^{-1}$ based on *total* generated glutathione conjugates). Kinetics and regio/stereoselectivity of rat CYP2F4 were indistinguishable from mouse CYP2F2. These results, combined with our recent immunomapping studies demonstrating minimal pulmonary CYP2F expression in rats, indicate that CYP2F expression is the factor most clearly associated with susceptibility to naphthalene-induced pneumotoxicity. CYP2F4 failed to display an enhanced ability to bioactivate 1-nitronaphthalene, an ability that could have potentially compensated for the lower CYP2F pulmonary expression levels in the rat, yet equal species susceptibilities. These results suggest the importance of other P450 enzymes in the epoxidation/bioactivation of 1-nitronaphthalene. Expression of recombinant CYP2F1 (human) yielded an immunoreactive protein with no detectable CO-difference spectrum suggesting inadequate heme incorporation.

The environmental toxicant naphthalene can be found in ambient air, ground water, sidestream and mainstream cigarette smoke, and in byproducts from the combustion of diesel fuel (Agency for Toxic Substances and Disease Registry, 1995). The results of the National Toxicology Program 2-year inhalation studies in mice and rats have found naphthalene to be associated with neoplasia in both species. The lifetime inhalation studies in mice demonstrated slightly increased incidences of alveolar/bronchiolar adenomas only in females at the highest concentration (30 ppm) (National Toxicology Program, 1992). In rats, however, neoplasms were confined to the nasal respiratory epithelium and the incidences were concentration-dependent (National Toxicology Program, 2000). Inhalation of naphthalene vapor at levels of 2 ppm and above leads to necrosis of murine pulmonary

bronchiolar epithelial cells (West et al., 2001). This exposure concentration is considerably lower than the current Occupational Safety and Health Administration standard (10 ppm, 8-h time-weighted average). These and other data were employed in the International Agency for Research on Cancer (IARC) classification of naphthalene as a possible human carcinogen (IARC Working Group, 2002). Like naphthalene, 1-nitronaphthalene (1-NN) poses a potential threat to human health. 1-Nitronaphthalene is generated in the atmosphere as a gas phase reaction product from naphthalene and N_2O_5 . Furthermore, the nitro- and methylnitronaphthalenes are thought to account for a major fraction of the mutagenic potential associated with air toxicants in the southern California air basin (Grosinsky et al., 1999). The extent to which naphthalene and 1-NN are found in the environment, the likelihood of human exposure, and the body of evidence demonstrating toxicity in animal models support the need to understand the mechanisms of toxicity for these compounds.

Naphthalene is metabolized to naphthalene 1,2-epoxide, a reactive intermediate, by the P450 system. Both the 1*S*,2*R*- and the 1*R*,2*S*-stereoisomers are produced. This biotransfor-

This work was supported by National Institute of Environmental Health Sciences Grants ES08408, ES04311, ES04699, and National Center for Research Resources Grant RR00169.

Article, publication date, and citation information can be found at <http://jpet.aspetjournals.org>.
doi:10.1124/jpet.104.075440.

ABBREVIATIONS: 1-NN, 1-nitronaphthalene; P450, cytochrome P450; rCYP2F, recombinant CYP2F; GST, glutathione S-transferase; bp, base pair(s); ORF, open reading frame; PCR, polymerase chain reaction; ALA, 5-aminolevulinic acid; FC, ferric citrate; CHAPS, 3-[(3-cholamidopropyl)dimethylammonio]-1-propanesulfonate; HPLC, high-pressure liquid chromatography; CDNB, 1-chloro-2,4-dinitrobenzene.

mation is the first and obligate step in the cascade of events leading to injury. Microsomes or airway explants from lungs of mice metabolize naphthalene with a high degree of stereoselectivity with ratios of 1*R*,2*S*- to 1*S*,2*R*-epoxide of 10:1 and >25:1, respectively (Buckpitt et al., 1992, 1995). Consistent with the lack of observable in vivo respiratory tract injury, both the absolute rate and the degree of stereoselectivity of naphthalene epoxidation are significantly less in rats than in mice. In contrast to the species selective toxicity observed with naphthalene, 1-NN is a potent lung toxicant in both mice and rats. P450-mediated bioactivation is essential to the toxicity of 1-NN (Verschoyle et al., 1993). Incubations of lung microsomal proteins from mice and rats display strikingly similar abilities to generate epoxides of 1-NN with the 7,8-epoxide predominating (Watt and Buckpitt, 2000).

Previous work demonstrated the presence of CYP2F2 in murine Clara cells correlates with the stereoselectivity and rate of naphthalene metabolism and with the site of injury (Buckpitt et al., 1995). Coincubation of an inhibitory CYP2F2 antibody dramatically decreases the formation of the 1*R*,2*S*-naphthalene oxide in murine lung microsomal incubations (Nagata et al., 1990). Recombinant CYP2F2 (rCYP2F2) metabolizes naphthalene rapidly and stereoselectively to the 1*R*,2*S* isomer, strongly suggesting the generation of this metabolite to be an important determinant of susceptibility (Shultz et al., 1999). In addition, rCYP2F2 metabolized 1-NN with a higher K_m and lower V_{max} than naphthalene; K_m and V_{max} values for 1-NN were 21 μ M and 17 min⁻¹, respectively. 1-NN-7,8-Epoxide was the predominate metabolite generated (Shultz et al., 2001). These data demonstrate the role of CYP2F in the initial bioactivation of these compounds. Given that rats and mice have comparable phase II detoxification systems (Lorenz et al., 1984), this unique combination of species susceptibilities are potentially attributable to 1) differences in the catalytic activities between mouse and rat CYP2F orthologs, 2) species differences in cellular CYP2F expression levels, or 3) a combination of these two factors.

Recent quantitative immunomapping studies of respiratory tract CYP2F expression have demonstrated profound differences between mice and rats correlating both with rates of in vitro naphthalene metabolism and with airway selective susceptibility (Baldwin et al., 2004). Although these results provide a reasonable explanation for differences in susceptibility to naphthalene-induced injury in rats and mice, they do not exclude the possibility that large catalytic activity differences may play a role as well. Studies comparing the metabolism of 3-methylindole by CYP2F orthologs from goat (CYP2F3) and human (CYP2F1) showed striking interspecies differences in catalytic activities of these proteins (Wang et al., 1998; Lanza et al., 1999). Similarly, recent work comparing the catalytic activities of recombinant mouse (rCYP2F2), goat (rCYP2F3), and rat (rCYP2F4) in the metabolism of dichloroethylene demonstrated relatively large differences in K_m and V_{max} values (Simmonds et al., 2004). To compare directly the capabilities of mouse and rat CYP2F isoforms to generate naphthalene and 1-nitronaphthalene epoxides, we have cloned and expressed a CYP2F isoform from rat lung (CYP2F4) using a baculovirus expression system. Furthermore, efforts to express rCYP2F1 (human) using systems identical to those used to generate catalytically active rCYP2F2 and rCYP2F4 yielded a recombinant protein

with no apparent incorporation of heme and little capacity to metabolize naphthalene.

Materials and Methods

Animals. Adult male Sprague-Dawley rats (225–250 g) were purchased from Charles River Laboratories, Inc. (Wilmington, MA). The animals were housed in an Association for Assessment and Accreditation of Laboratory Animal Care-accredited facility in cage racks supplied with high-efficiency particulate-filtered air and inert bedding. Animals had free access to food (Purina Rodent Chow) and water with a 12-h/12-h light/dark cycle for at least 7 days before use. Rodents were killed with an overdose of sodium pentobarbital administered i.p.

Reagents. The mouse CYP2F2 cDNA clone in pBluescript SK– was a gift from Dr. J. Ritter (Medical College of Virginia, Richmond, VA). Recombinant CYP2F2 was previously produced in our laboratory (Shultz et al., 1999). *Spodoptera frugiperda* (Sf9) and *Trichoplosia ni* (Tn5) cells were obtained from American Type Culture Collection (Manassas, VA) and Invitrogen (Carlsbad, CA), respectively. Ex-Cell 405 medium was purchased from JRH Biosciences (Lenexa, KS). Rat NADPH cytochrome P-450 oxidoreductase (reductase) was purified from rat liver using standard procedures (Strobel and Dignam, 1978). Reductase was quantified by the standard cytochrome *c* reduction assay (Guengerich, 1994). Glutathione *S*-transferase (GST) from mouse liver cytosol was purified by standard procedures using affinity column chromatography (Simons and Vander Jagt, 1981), and activities were assessed with 1-chloro-2,4-dinitrobenzene as substrate. Unless otherwise stated, all other reagents were purchased from commercial vendors and were of reagent/analytical grade.

Construction of Rat Lung cDNA Library and Isolation of Rat CYP2F4. Lungs from four rats were perfused with saline, quickly removed, and then flash frozen in liquid nitrogen. Frozen sections of approximately 100 mg were used to isolate total RNA (RNeasy Mini; QIAGEN, Valencia, CA) from each rat. Total RNA was pooled, and poly(A)⁺ RNA was affinity purified on an oligo(dT)-cellulose column. Prior to cDNA library construction, 3 μ g of poly(A)⁺ RNA was subjected to northern blot analysis using a ³²P-labeled cDNA probe containing approximately 1400 bp of the mouse CYP2F2 open reading frame (ORF) to verify the presence of a cross hybridizing transcript of the appropriate length in rat lung (results not shown). Double-stranded cDNA was synthesized from poly(A)⁺ RNA and directionally ligated to the bacteriophage vector λ ZAP using a cDNA synthesis kit (ZAP-cDNA synthesis kit; Stratagene, La Jolla, CA). Recombinant phage-infected XL1-Blue MRF' cells were screened with the ³²P-labeled cDNA probe used previously for northern analysis, and pBluescript phagemid was excised from positive plaques. Using a combination of restriction digestion and direct sequencing (Applied Biosystems, Foster City, CA), several clones were found to contain cDNA from a CYP2F2 ortholog, two of which contained the entire ORF. The two full-length clones were bidirectionally sequenced and the consensus sequence (CYP2F4) was submitted to the P450 nomenclature committee and then GeneBank (accession no. AF017393).

Expression of Recombinant CYP2F4 and CYP2F1. The cDNA insert encoding rat CYP2F4 (0–1776 bp) was excised from pBluescript SK– using the EcoRI and XhoI cleavage sites and directionally cloned into the multiple cloning site of pFastBac1 (Invitrogen). The integrity and orientation of the pFastBac/2F4 clone was verified by bidirectional sequencing. The cDNA encoding CYP2F4 from pFastBac1/2F4 was site-specifically transposed into the baculovirus genome as described in the manufacturer's protocol (Bac-to-Bac Expression System; Invitrogen). The high molecular weight genomic DNA was purified from recombinant clones and used to transfect Sf9 cells for the production of baculovirus stocks.

Human lung tissue was obtained via Golden State Organ Donor Services (Sacramento, CA) and used to isolate total RNA (RNeasy

Mini; QIAGEN). To clone the CYP2F1 ORF, RNA was reverse-transcribed (Superscript II; Invitrogen) using a poly(A) primer followed by PCR amplification (Turbo PFU; Stratagene) of the single-stranded cDNA using a forward primer containing a BclI cleavage site (5'-gggcgctgataaccATGgacagcataagcacag-3') and a reverse primer containing a HindIII cleavage site (5'-atcgtaaagcttgT-**T**Aggcggggcagg-3'). The PCR product was purified (QIAquick PCR purification kit; QIAGEN), restriction digested with BclI and HindIII, and then directionally cloned into the BamHI and HindIII sites of the pFastBac1 transfer vector multiple cloning site. The cloned CYP2F1 cDNA was bidirectionally sequenced and found to be identical to the CYP2F1 mRNA RefSeq (NM_000774). Recombinant CYP2F1 baculovirus stocks were prepared in an identical fashion to CYP2F4.

Baculovirus stocks were amplified in Sf9 cells and viral titer was obtained using a BacPAK Baculovirus Rapid Titer kit (BD Biosciences Clontech, Palo Alto, CA). Tn5 cells grown as monolayers in complete Ex-Cell 405 were used to optimize expression and produce active enzyme. Infections were performed by incubating virus with the cells in the presence of 100 μ M 5-aminolevulinic acid (ALA) and 100 μ M ferric citrate (FC). Cell lysates were prepared by pelleting cells at 1000g for 10 min followed by three washes with ice-cold phosphate-buffered saline and resuspension in 0.1 M phosphate buffer, pH 7.4, with 20% glycerol and protease inhibitors (Cocktail Set III; Calbiochem, San Diego, CA). Cells were lysed with two 10-s rounds of sonication on ice followed by centrifugation at 1000g for 10 min to remove unlysed cells. When spectrally active recombinant protein was obtained, cell lysate spectral activity per milligram of protein was used as an endpoint to optimize multiplicity of infection and viral incubation time. P450 levels were determined by obtaining difference spectra of sodium dithionite-reduced versus CO-bubbled samples at 500 to 400 nm according to Omura and Sato (1964). Alternatively, in the case of CYP2F1 where spectrally active protein was unobtainable, immunoblot analysis was used as a surrogate endpoint. Proteins from Tn5 cell lysates were separated by SDS-polyacrylamide gel electrophoresis using 1-mm 10% BisTris gels (Invitrogen). Bands were visualized by SYPRO Ruby staining (Molecular Probes, Eugene, OR). To determine relative protein abundances, SYPRO Ruby-stained gels were scanned on a Typhoon 8600 scanner, using a 532-nm excitation wavelength and a 610BP30 emission filter. Immunoblots using a rabbit polyclonal anti-CYP2F2 antibody (Nagata et al., 1990) were performed as described previously (Baldwin et al., 2004).

To serve as a positive control during rCYP2F1 expression studies, rCYP2F4 viral stocks were used concurrently, and reagents were pooled wherever possible. To address the possibility that rCYP2F1 was more labile than rCYP2F4, a subpopulation of viral-infected Tn5 cells were harvested and lysed using only glass-glass homogenization without sonication. Additionally, after the Tn5 cells were centrifuged to harvest recombinant protein, DNA was isolated (Plasmid Mini kit, QIAGEN) from an aliquot of the virus-containing cell culture media supernatant. Using primers flanking the transposition site in the viral genome (M13 forward and reverse), the transposed pFastBac1 sequence was PCR amplified using a polymerase with high fidelity and processivity (Herculase; Stratagene). After removal of unincorporated nucleotides and primers (QIAquick PCR purification kit; QIAGEN) the \approx 1500 base region containing either the CYP2F1 or CYP2F4 ORF within the \approx 4-kilobase amplicon was sequenced to verify the gene sequence of the CYP2F baculoviruses and to rule out the possibility of viral cross contamination.

Measurement of Naphthalene and 1-Nitronaphthalene Metabolism. The rates of naphthalene metabolism were determined in incubations containing recombinant CYP2F4 (quantity determined spectrally), reductase (quantified by cytochrome *c* activity), NADPH-regenerating system (0.25 U glucose-6-phosphate dehydrogenase, 14 mM glucose 6-phosphate, 2.18 mM NADP, and 1 mM $MgCl_2$), 1 mM glutathione, GST (amount specified in figure legends), and 2 mM CHAPS in a total volume of 250 μ l (0.1 M Na_2HPO_4 , pH 7.4). The

ratio of reductase to CYP2F4 (units/picomole) as well as the concentration of CHAPS detergent were optimized for greatest enzyme activity for each substrate and used for all kinetic determinations. Glutathione and GST were included for the trapping of reactive epoxides as stable glutathione conjugates. Enzyme incubations and the separation of glutathione conjugates by reversed-phase HPLC

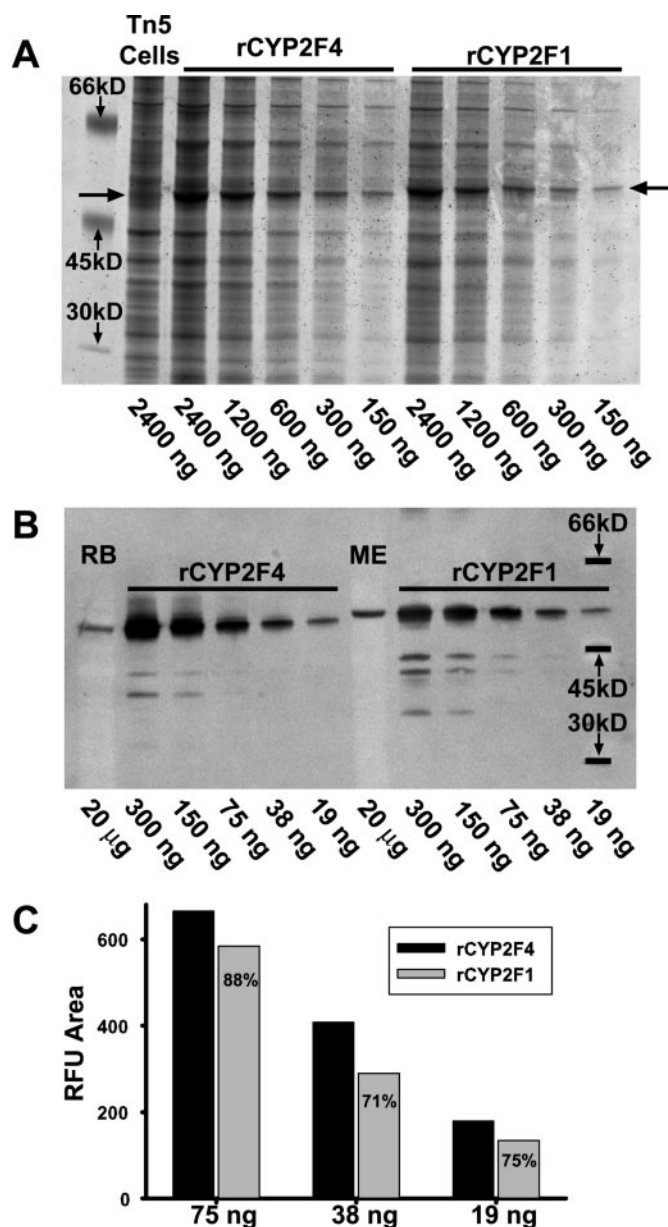


Fig. 1. A, SYPRO Ruby-stained 10% polyacrylamide gel of proteins recovered from CYP2F4- and CYP2F1-infected Tn5 insect cell lysates. Arrows denote protein bands associated with the expressed CYP2F isoforms. Noninfected Tn5 cells are shown for comparison. Nanogram amounts listed refer to total cellular protein applied to the gel. B, immunoblot analysis of proteins detected in insect cell lysates infected with CYP2F4 and CYP2F1 baculovirus. Except where noted otherwise, values reflect nanogram amounts of total cellular protein applied to the gel. Samples of rat terminal bronchiole postmitochondrial supernatants (RB) along with microsomes from rhesus macaque ethmoid nasal epithia (ME) were included as positive controls. C, relative fluorescence unit (RFU) areas of immunoblot protein bands associated with expressed CYP2F (protein samples outside of linear range omitted). Bands were quantified using ImageQuant 5.2 software (Amersham Biosciences Inc., Piscataway, NJ) for comparison of relative rCYP2F expression levels. The numbers in the light gray bars refer to the percentage of rCYP2F1 relative fluorescence unit area compared with rCYP2F4.

with quantification by UV absorption were performed as described previously (Shultz et al., 1999).

Using conditions optimized for maximal naphthalene turnover with rCYP2F4, the activity of Tn5 cell lysates containing rCYP2F1 was studied. Cell lysates and cofactors were incubated with 1 mM naphthalene at 37°C for 20 min. Given the absence of spectral activity, comparisons of rCYP2F1 and rCYP2F4 naphthalene metabolism were standardized based on total amounts of cell lysate protein in each incubation. Similar levels of immunoreactive CYP2F per milligram of cell lysate protein for both isoforms justified this approach (Fig. 1, B and C). Given the anticipated low or nonexistent levels of naphthalene metabolism, lysates from both noninfected and wild-type baculovirus-infected Tn5 cells were used as negative controls. Additionally, in several enzyme incubations the amount of reductase was varied independently as a means to rule out any metabolic contribution arising from the reductase preparation.

Incubations with 1-NN were carried out in 250- μ l volumes with amounts of recombinant CYP2F4, reductase, and other cofactors optimized for maximal 1-NN turnover as described above. Glutathione conjugates were separated by HPLC and measured by UV absorption at 256 nm according to established methods (Watt et al., 1999). Quantification of 1-NN conjugates was based on the preparation of 14 C-labeled standards. [14 C]1-NN (1 mM) was incubated with rat liver microsomes for 10 min at 37°C. Methanol extracts of the incubation mixture were evaporated to dryness and reconstituted for HPLC analysis. Fractions of the column eluate were collected at 15-s intervals and radioactivity counted with a Beckman LS5000TD scintillation counter. Peak areas at 256 nm for each of the metabolite peaks were compared with total disintegrations per minute for the peak to obtain peak area per nanomole ratios. These ratios were subsequently used to determine metabolite quantities in incubations with unlabeled substrate.

Results

Cloning and Expression of CYP2F4 and CYP2F1. Using rat lung total RNA for northern analysis, a gene transcript of \approx 1900 bp was found to hybridize with a mouse CYP2F2 probe under stringent conditions (data not shown). Accordingly, the rat ortholog of CYP2F2 was cloned from a lung cDNA library. The consensus sequence of the novel gene derived from two full-length clones was 1768 bp and contained 12 bp of 5'UTR. The deduced amino acid sequence of CYP2F4 (accession no. AF017393) showed a homology of 94% with CYP2F2 and 81% to CYP2F1. This novel P450 was then expressed in insect cells using the baculovirus expression system. As in previous work, Tn5 cells were found to yield higher amounts of recombinant protein compared with Sf9 cells. A major cellular protein with an apparent molecular weight of 50 to 52 kDa was present in lysates of Tn5 cells infected 84 h earlier with baculovirus containing CYP2F4 (Fig. 1A). Immunoblot analysis of lysate proteins confirmed the presence of a protein recognized by a polyclonal antibody generated to CYP2F2, comigrating with the immunoreactive band observed in rat terminal bronchioles (Fig. 1B). A typical yield of spectrally active CYP2F4 was 260 pmol/mg cell lysate protein.

Incubation of Tn5 cells with the CYP2F1 baculovirus produced significant amounts of recombinant protein as visualized in SYPRO Ruby-stained gels (Fig. 1A). Immunoblot analysis of Tn5 cell lysates and microsomes prepared from the rhesus macaque ethmoid nasal epithelium, the respiratory tract subcompartment with the greatest CYP2F abundance, using an antibody generated to CYP2F2 demonstrated comigration of immunoreactive proteins (Fig. 1B). Compar-

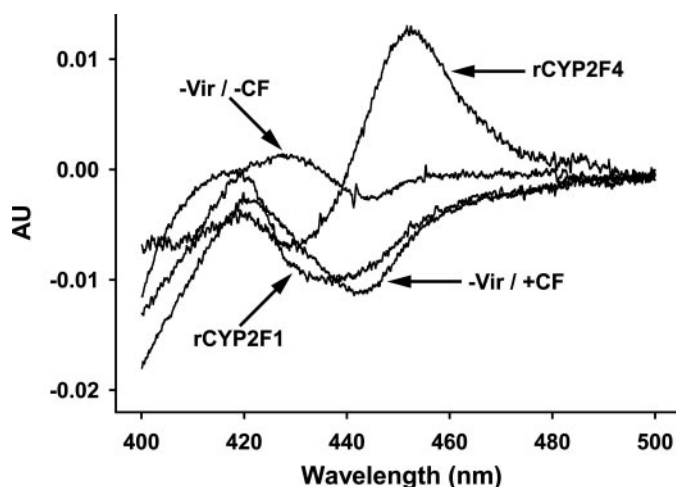


Fig. 2. Sodium dithionite-reduced, CO-difference spectra for lysates of CYP2F4- and CYP2F1-infected Tn5 insect cells. Infected cells were supplemented with ALA/FC (CF). Supplemented (-Vir/+CF) and nonsupplemented (-Vir/-CF) uninfected Tn5 cells are shown as controls.

able amounts of immunoreactive rCYP2F1 and rCYP2F4 apoprotein were produced in Tn5 cells infected in parallel when data were normalized per nanogram of cell lysate protein (Fig. 1C). Multiple experiments demonstrated CO-difference spectra for ALA/FC supplemented rCYP2F1 which were not discernibly different from spectra obtained from lysates of supplemented noninfected cells (Fig. 2). Substitution of glass-glass homogenization for sonication of cell pellets from either CYP2F4 or CYP2F2 baculovirus-infected cells resulted only in a significant decrease in the amount of immunoreactive CYP2F protein per milligram of cell lysate protein and in the case of rCYP2F4, a reduction in P450 levels determined spectrally. Sequence analysis of CYP2F1 and CYP2F4 baculoviruses during expression demonstrated the absence of any mutations.

Measurement of Naphthalene and 1-Nitronaphthalene Metabolism. Prior to the determination of the catalytic activity of rCYP2F4, incubation conditions and cofactor concentrations were optimized for maximal naphthalene turnover as described previously for rCYP2F2 (Shultz et al., 1999). The concentration of detergent (CHAPS) in the incu-

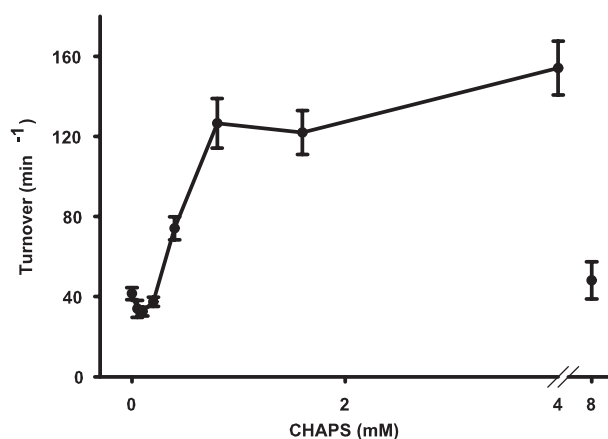


Fig. 3. Optimization of CHAPS concentration for maximal turnover of naphthalene by rCYP2F4. Ten-minute incubations containing 2.2 pmol rCYP2F4, 800 μ M naphthalene, 240 units of reductase, 1 mM glutathione, 2.5 CDNB units GST, and NADPH-generating system. Values are mean \pm S.D., $n = 3$.

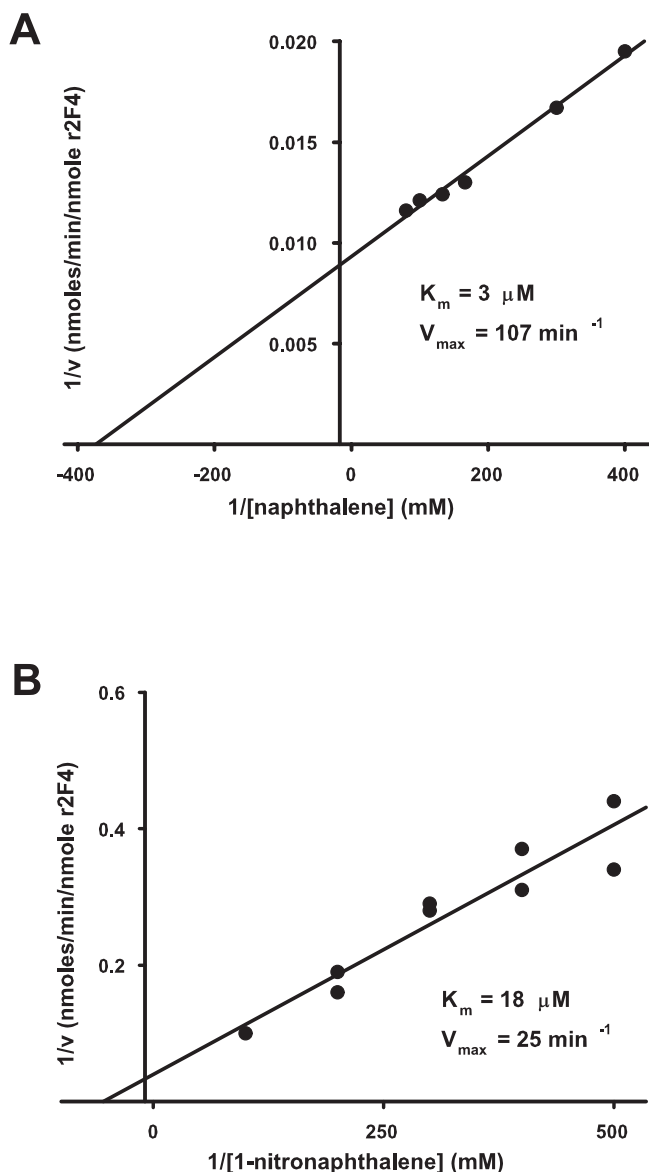


Fig. 4. Double reciprocal plots for the determination of the apparent K_m and V_{max} values for naphthalene and 1-nitronaphthalene metabolism by recombinant CYP2F4. A, naphthalene: 6-min incubations containing rCYP2F4 (2.2 pmol), 240 units of reductase, NADPH-regenerating system, 2.5 CDNB units GST, 1 mM glutathione, 2 mM CHAPS, and naphthalene. B, 1-nitronaphthalene: 10-min incubations containing rCYP2F4 (2.6 pmol), 240 units of reductase, NADPH-regenerating system, 2.5 CDNB units GST, 1 mM glutathione, 2 mM CHAPS, and 1-nitronaphthalene.

TABLE 1

Comparison of recombinant CYP2F catalytic activities

Summary of the CYP2F4 and CYP2F2 kinetic parameters for naphthalene and 1-nitronaphthalene metabolism.

Isoform	K_m	V_{max}	7,8:5,6 Epoxides	1R,2S:1S,2R
	μM	min^{-1}		
Naphthalene metabolism				
rCYP2F2*	3	104		66:1
rCYP2F4	3	107		>50:1
1-Nitronaphthalene metabolism				
rCYP2F2*	21	17	5:1	
rCYP2F4	18	25	20:1	

* Data taken from Shultz et al., 1999 and 2001 for comparison.

bation was found to significantly affect the rate of naphthalene metabolism; increasing the CHAPS concentration to 8 mM resulted in a precipitous, 70% reduction in maximal enzyme activity (Fig. 3). Based on these results, a concentration of 2 mM was used for all further studies. Preliminary studies directly comparing catalytic activities of rCYP2F4 and rCYP2F2 using saturating naphthalene concentrations (0.5–1.0 mM) revealed nearly identical maximal catalytic activities and stereoselectivities (data not shown). For further studies with rCYP2F4, the linearity of product formation with incubation time and enzyme concentration was determined, and all incubations were conducted in the linear portions of these curves. Incubations were performed for either 4 or 6 min using substrate concentrations ranging from 2 μM to 2 mM. Reciprocals ($1/v$ versus $1/S$) were plotted, and intercepts were calculated by linear regression analysis (Fig. 4). Values for K_m and V_{max} are shown in Table 1. The ratio of 1R,2S/1S,2R epoxides inferred from the glutathione conjugates was >50:1.

Incubations of naphthalene with rCYP2F1 yielded rates of naphthalene metabolism per milligram of cell lysate protein ranging from 100- to 900-fold less than identical incubations using rCYP2F4. Activities with rCYP2F1 were never statistically different from those of either negative control (Table 2). Although the differences were not statistically significant, it appeared that total naphthalene metabolism was more sensitive to changes in the amount of reductase than to the amount of recombinant CYP2F1 protein (Table 2). A metabolism scheme along with representative chromatograms of extracts prepared from incubations of rCYP2F1 and rCYP2F4 with naphthalene are shown in Fig. 5. Based on our inability to detect any metabolic activity associated with rCYP2F1, no further metabolic studies were performed with rCYP2F1.

Assay conditions, cofactors, and linearity with time and enzyme concentration were independently optimized with CYP2F4 for maximal turnover of 1-NN. Incubations were conducted for 10 min at substrate concentrations of 2 to 200 μM . Recombinant CYP2F4 metabolized 1-NN to both the 5,6- and 7,8-epoxide intermediates that were trapped and quantified as glutathione conjugates. The identity of these metabolites was established by comigration with purified standards whose identity and regiochemistry were established by mass spectroscopy and NMR (Watt et al., 1999). Figure 6 shows the structures and scheme of 1-NN metabolism, as well as the corresponding peaks on HPLC. The predominant conjugates detected were metabolites 1, 2, 3, 4, and 6 corresponding to a 20:1 ratio of 7,8-epoxide to 5,6-epoxide. The K_m and V_{max} for the conversion of 1-NN to glutathione conjugates are shown in Table 1.

Discussion

A number of pulmonary toxicants, including naphthalene, show highly species-selective toxicity. Administration of naphthalene at doses as low as 50 mg/kg i.p. produces detectable Clara cell necrosis in mice; toxicity is not discernable in rat lungs even at doses of 1600 mg/kg (Plopper et al., 1992). These species differences in susceptibility correlate well with the rate of metabolism of naphthalene to epoxides in both lung microsomes (Buckpitt et al., 1992) and in dissected airway explants (Buckpitt et al., 1995). Furthermore,

TABLE 2

Naphthalene metabolism in insect cell lysates^a

Naphthalene turnover in cell lysates containing either rCYP2F4 or rCYP2F1. Lysates from uninfected (–Virus) or wild-type (WT) baculovirus-infected Tn5 cells (both supplemented with ALA/FC) were used to control for potential metabolism unassociated with either rCYP2F enzyme. Twenty-minute incubations contained 1 mM naphthalene, 400 U of reductase, 1 mM glutathione, 5 CDNB units GST, 2 mM CHAPS, NADPH-regenerating system, and varying amounts of insect cell lysate protein. To serve as an additional control, lysates from uninfected cells (100 μg) were combined with varying amounts of reductase (200, 400, and 600 U). Results shown are femtomoles of naphthalene glutathione conjugates derived from epoxide isomers/micrograms of cell lysate protein/minute.

	Micrograms of Cell Lysate Protein	1 <i>R</i> ,2 <i>S</i> -Epoxide	1 <i>S</i> ,2 <i>R</i> -Epoxide	Turnover	Ratio 1 <i>R</i> ,2 <i>S</i> /1 <i>S</i> ,2 <i>R</i>
		<i>fmol/μg/min</i>		<i>pmol/pmol/min</i>	
rCYP2F4	50	5837 ± 693	100 ± 23	95 ± 11	59 ± 8
	100	6851 ± 600	96 ± 12	116 ± 9	72 ± 3
	200	6820 ± 162	112 ± 5	116 ± 3	61 ± 3
rCYP2F1	50	51 ± 10	26 ± 2	**	1.9
	100	31 ± 2	12 ± 1	**	2.5
	200	8 ± 3	3 ± 2	**	2.5
WT virus	50	48 ± 5	23 ± 1	**	2.1
	100	25 ± 6	11 ± 3	**	2.3
	200	12 ± 3	6 ± 1	**	2.2
–Virus	50	51 ± 4	23 ± 2	**	2.2
	100	26 ± 6	12 ± 1	**	2.1
	200	6 ± 2	5 ± 4	**	1.2
–Virus 100 μg (<i>n</i> = 3)	200*	24 ± 2	13 ± 4	**	1.9
	400*	27 ± 6	16 ± 4	**	1.7
	600*	36 ± 12	19 ± 3	**	1.9

^a Values are the mean ± S.D. for four separate incubations.

* Reductase units.

** Indeterminable due to absence of spectrally quantifiable P450 levels.

there are no striking differences in either pulmonary epoxide hydrolase- or GST-mediated detoxification pathways for naphthalene oxide, which would account for the unusual susceptibility of the mouse compared with the rat (Lorenz et al., 1984). Generation of naphthalene oxide, the first and obligate step in the cascade of events leading to injury, is mediated by CYP2F, making this enzyme a key factor in the species susceptibility of this compound (Warren et al., 1982; Ritter et al., 1991). The observed differential in rates of naphthalene activation across species and within the respiratory tract is likely attributable to differences in CYP2F expression, catalytic activity, or a combination of both factors. Recombinant mouse CYP2F2 generates naphthalene oxide with high catalytic efficiency and stereoselectivity, supporting its role in the generation of reactive metabolites in this species (Shultz et al., 1999). Recent quantitative immunoblot studies showed significant differences in CYP2F expression between mice and rats (Baldwin et al., 2004). These findings are consistent with the view that enzyme expression accounts, at least partially, for differences in susceptibility to naphthalene toxicity. The current work revealed that rat CYP2F4 generates naphthalene and 1-NN epoxides with catalytic activities and stereoselectivities nearly identical to the mouse isoform. These findings indicate that CYP2F expression is closely associated with susceptibility to naphthalene-induced injury and that limited expression of CYP2F is sufficient to confer resistance in rats. Studies of heterologously expressed CYP2F1 demonstrated significant yields of immunoreactive, yet spectrally inactive, recombinant protein thus suggesting the generation of the apoprotein but not the holoenzyme. As expected, this protein had only a very limited ability to catalyze the conversion of naphthalene to naphthalene-oxide, indiscernible from negative controls.

If CYP2F4 were a major contributor to the metabolism of naphthalene in vivo, then the catalytic activity and high degree of stereoselectivity for naphthalene epoxidation demonstrated by rCYP2F4 should be reflected by high substrate turnover and high ratios of 1*R*,2*S*- to 1*S*,2*R*-epoxide within

the respiratory tract. Airway subcompartments microdissected from rat lung generate naphthalene oxide at relatively low rates and the 1*S*,2*R*-epoxide is the major metabolite. These data indicated a negligible contribution from CYP2F4 in these areas of the respiratory tract (Buckpitt et al., 1995). Data obtained with rat nasal epithelium is strikingly different, displaying significant naphthalene turnover with more than a 30-fold ratio of 1*R*,2*S*- to 1*S*,2*R*-epoxide in the olfactory epithelium (Buckpitt et al., 1992). The highest rates of naphthalene turnover were found in the olfactory epithelium, followed by the lateral wall (2-fold less) and the septum (9-fold less). Immunoblot studies quantitating the relative differences in CYP2F4 expression within the rat respiratory tract have defined a distribution pattern nearly identical to the patterns of 1*R*,2*S* generation (Baldwin et al., 2004). These data suggest that CYP2F4 expression is proportional to 1) the amount of 1*R*,2*S*-epoxide generated, and 2) the extent of naphthalene-induced injury observed in vivo. Therefore, the most important factor in determining tissue susceptibility to naphthalene injury in the rat appears to be the level of CYP2F4 expression.

Previous studies in mice and rats using 1-NN have demonstrated similar in vivo cytotoxicities (Rasmussen et al., 1986; Sauer et al., 1997). Furthermore, in vitro incubations of lung microsomal proteins have shown strikingly similar rates of substrate epoxidation with the 7,8-epoxide predominating in both species (Watt and Buckpitt, 2000). Prior characterization of rCYP2F2 and the preponderance of 1-NN glutathione conjugates 2 and 4 (arising from the 7,8-epoxide) in mouse lung incubations supports the involvement of CYP2F2 in the metabolism of 1-NN in this tissue, a finding that is consistent with recent immunoblot studies (Baldwin et al., 2004). Conversely, the current studies showing rCYP2F4 to strongly favor the generation of 1-NN glutathione conjugates 2 and 4 and the nearly equal amounts of 1-NN glutathione conjugates 1, 3, and 4 (from both 5,6- and 7,8-epoxides) observed in lung microsomal incubations support the involvement of other P450 isoform(s) in the bioactivation

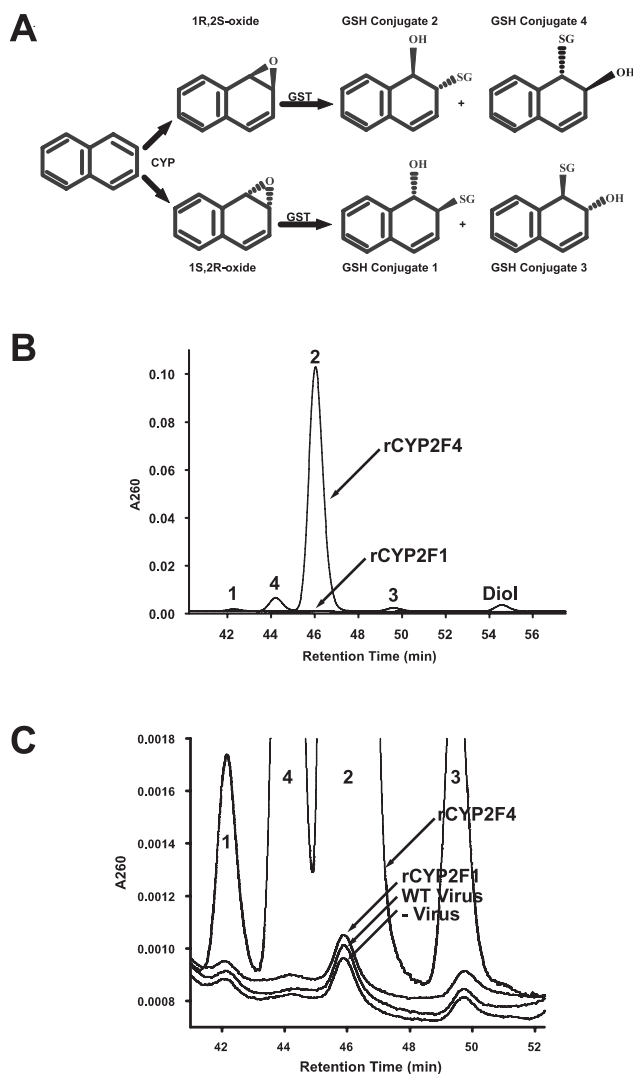


Fig. 5. A, metabolism scheme of naphthalene to form the 1,2-naphthalene oxides and the resultant glutathione conjugates (numbered according to convention of Buckpitt et al., 1987). B, HPLC UV chromatographic separation of naphthalene glutathione conjugates generated from incubations of insect cell lysates containing either rCYP2F4 or rCYP2F1. C, lysates from both uninfected (-Virus) and wild-type baculovirus (WT Virus)-infected cells supplemented with ALA/FC were used to control for potential metabolism unassociated with either rCYP2F enzyme. Glutathione conjugates, along with naphthalene dihydrodiol (diol), are labeled above the associated HPLC UV absorbance peaks.

of 1-NN in the lungs of rats. These findings are consistent with the conclusions of Verschoyle and coworkers who suggested that the bioactivation of 1-NN were catalyzed by CYP2B in rat lung (Verschoyle et al., 1993).

Data on CYP2F1 expression in human tissue are limited with the majority of studies utilizing reverse transcriptase-PCR techniques to detect CYP2F1 transcript. With the exception of the lung and placenta, all other human tissues tested have no detectable levels of CYP2F1 mRNA (Hakkola et al., 1996; Andersen et al., 1998; Nishimura et al., 2003). Assessment of CYP2F1 transcript levels in the respiratory tract has been limited to homogenates of whole lung. Therefore, expression levels within discrete areas of the conducting airways or nasal epithelium are unknown. Direct evidence for CYP2F1 protein in the human lung is also lacking, but recent work in rhesus macaques using an antibody to

CYP2F2 showed undetectable amounts of protein in all segments of the respiratory tract except the ethmoid nasal epithelium (Baldwin et al., 2004). Despite an incomplete understanding of the expression of CYP2F1 in the human respiratory tract, the value of determining enzyme expression levels is contingent on the existence of a catalytically active protein.

The ability of human CYP2F1 to generate naphthalene oxide remains equivocal. Initial studies using a vaccinia-virus system to express recombinant CYP2F1 yielded small amounts of protein, necessitating 6-h incubations to detect metabolites (Thornton-Manning et al., 1996). The profile of 3-methylindole metabolites generated differed substantially from those obtained using rCYP2F3 (Wang et al., 1998). In an attempt to address these issues, Lanza et al. (1999) utilized a lymphoblastoid system to express spectrally quantifiable amounts of rCYP2F1 to further study the kinetics of 3-methylindole and naphthalene metabolism. Saturating concentrations of naphthalene (500 μ M) and large amounts of rCYP2F1 (240 pmol/incubation) yielded levels of naphthalene conjugates near the analytical limit of detection with an 8-fold preference for the 1S,2R-epoxide. Maximal naphthalene turnover was 35.5 pmol/nmol P450/min or 0.036 min^{-1} , approximately 3000-fold lower than values obtained with rCYP2F4 or rCYP2F2.

Side by side expression studies of rCYP2F1 and rCYP2F4 yielded significant amounts of both proteins, each having the appropriate molecular weight and immunoreactivity. However, only rCYP2F4 produced a detectable reduced CO-difference spectra, indicating that heme was correctly incorporated in the rodent CYP2F but not in human CYP2F1. Although there are many examples of mutations that cause loss of function in human P450 isoforms (reviewed in Ingelman-Sundberg, 2002; <http://www.imm.ki.se/CYPalleles/>), the majority of these alterations are due to large deletions or point mutations causing splice-site, frameshift, or nonsense mutations and hence a protein product with an altered molecular weight. Given the multiple rounds of sequence verification, a mutation in the expressed CYP2F1 is unlikely. Several studies using heterologously expressed human P450 alleles containing a single missense mutation have demonstrated a complete loss of function as evidenced by the absence of both spectral and metabolic activity (Yamano et al., 1990; Evert et al., 1997). However, the precedent does exist for baculovirus-expressed P450 proteins to have no detectable CO-difference spectrum, yet measurable catalytic activity. Even though the spectrally inactive CYP2A6*6 allele is only 10% as active in coumarin hydroxylation as its wild-type counterpart, these activities were still well above (10-fold) controls (Kitagawa et al., 2001). This does not appear to be the case with CYP2F1 where detectable metabolic activities were indiscernible from negative controls.

As indicated earlier, previous studies in a lymphoblastoid expression system (Lanza et al., 1999) were able to measure small amounts of cytochrome P450 (20 pmol/mg microsomal protein). More recent studies, which used a cytomegalovirus-based viral vector to express CYP2F1 in a human bronchial epithelial cell line (BEAS-2B), have demonstrated the presence of recombinant protein by immunoblot analysis (Nichols et al., 2003; Sheets et al., 2004). Both studies demonstrated rCYP2F1 catalytic activity in BEAS-2B cells, inferred by either loss of cell viability with 3-methylindole incubation or

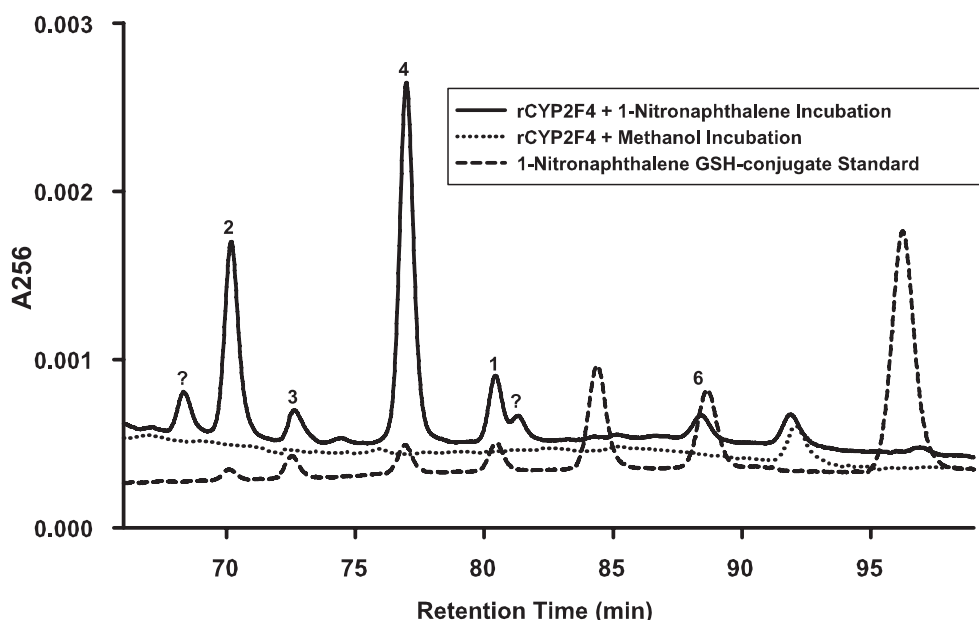
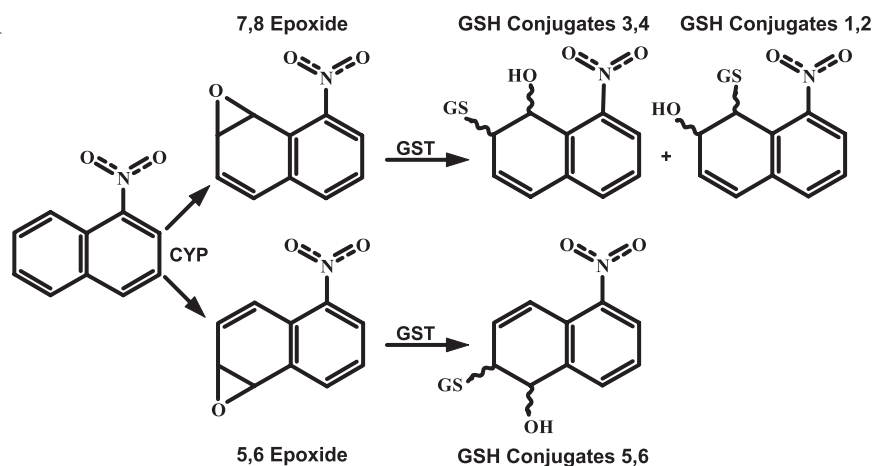


Fig. 6. Metabolism scheme of 1-nitronaphthalene to generate the 7,8- and 5,6-nitronaphthalene oxides and glutathione conjugates. HPLC UV profile of metabolites generated in a 10-min incubation containing rCYP2F4 (2.6 pmol), 240 units of reductase, NADPH-regenerating system, 2.5 CDNB units GST, 1 mM glutathione, 2 mM CHAPS, and 1-nitronaphthalene (1 mM). Incubations yielded five major metabolites which have been identified as the glutathione conjugates of the 7,8-epoxide (conjugates 1–4) and to a lesser extent the 5,6-epoxide (conjugate 6). The purified standards along with a negative control enzyme incubation (solvent alone) are shown for reference.

quantification of benzene metabolism. Benzene metabolism was relatively limited with an estimated V_{max} of 10 pmol/nmol P450/min. Thus, from the available data 1) functional CYP2F1 has been difficult to express, 2) rCYP2F1 does not incorporate heme properly in a baculovirus system which yields high levels of catalytically active rodent CYP2F proteins, and 3) when rCYP2F1 holoenzyme is expressed, relatively low rates of substrate metabolism are observed.

In summary, the data presented here demonstrate that rat rCYP2F4 metabolizes naphthalene and 1-NN with high catalytic activities and regioselectivity, nearly identical to mouse rCYP2F2. Therefore, the observed differences in species and respiratory distribution patterns of 1R,2S-epoxide generation and in vivo cytotoxicity are likely due to differences in levels of CYP2F expression. Low expression levels of CYP2F protein are sufficient to account for the insensitivity of rats to naphthalene-induced cytotoxicity. Extrapolation of these findings to humans and other primates would suggest that, given equally efficient phase II detoxification systems (Pacifi et al., 1981; Bryan and Jenkinson, 1987), a deficit in either CYP2F catalytic activity or expression levels would result in an insensitivity to naphthalene-induced injury. Al-

though relative expression data exist for the rhesus macaque, analogous data in the human is lacking. Future immunologic and/or proteomic studies could provide these comparative data. In addition, characterization of the multiple potential human CYP2F1 alleles identified from public genetic databases, along with CYP2F1/2F4 chimeras, should prove beneficial in determining regions critical in the expression of catalytically active protein.

Acknowledgments

The University of California at Davis is a National Institute of Environmental Health Sciences Center (05707), and support for core facilities used in this work is gratefully acknowledged.

References

- Agency for Toxic Substances and Disease Registry (ATSDR) (1995) *Toxicological Profile for Naphthalene, 1-Methylnaphthalene, 2-Methylnaphthalene*, pp 1–200. U.S. Department of Health and Human Services, Agency for Toxic Substances and Disease Registry, Atlanta, GA.
- Andersen MR, Farin FM, and Omiecinski CJ (1998) Quantification of multiple human cytochrome P450 mRNA molecules using competitive reverse transcriptase-PCR. *DNA Cell Biol* 17:231–238.
- Baldwin RM, Jewell WT, Fanucchi MV, Plopper CG, and Buckpitt AR (2004) Comparison of pulmonary/nasal CYP2F expression levels in rodents and rhesus macaque. *J Pharmacol Exp Ther* 309:127–136.

- Bryan CL and Jenkinson SG (1987) Species variation in lung antioxidant enzyme activities. *J Appl Physiol* **63**:597–602.
- Buckpitt AR, Buonarati M, Avey LB, Chang AM, Morin D, and Plopper CG (1992) Relationship of cytochrome P450 activity to Clara cell cytotoxicity. II. Comparison of stereoselectivity of naphthalene epoxidation in lung and nasal mucosa of mouse, hamster, rat and rhesus monkey. *J Pharmacol Exp Ther* **261**:364–372.
- Buckpitt AR, Castagnoli N Jr, Nelson SD, Jones AD, and Bahnson LS (1987) Stereoselectivity of naphthalene epoxidation by mouse, rat, and hamster pulmonary, hepatic and renal microsomal enzymes. *Drug Metab Dispos* **15**:491–498.
- Buckpitt AR, Chang AM, Weir A, Van Winkle L, Duan X, Philpot R, and Plopper C (1995) Relationship of cytochrome P450 activity to Clara cell cytotoxicity. IV. Metabolism of naphthalene and naphthalene oxide in microdissected airways from mice, rats and hamsters. *Mol Pharmacol* **47**:74–81.
- Evert B, Eichelbaum M, Haubruck H, and Zanger UM (1997) Functional properties of CYP2D6 1 (wild-type) and CYP2D6 7 (His324Pro) expressed by recombinant baculovirus in insect cells. *Naunyn-Schmiedeberg's Arch Pharmacol* **355**:309–318.
- Groszovsky AJ, Sasaki JC, Arey J, Eastmond DA, Parks KK, and Atkinson R (1999) Evaluation of the potential health effects of the atmospheric reaction products of polycyclic aromatic hydrocarbons. *Res Rep Health Eff Inst* **84**:1–22.
- Guengerich FP (1994) Analysis and characterization of enzymes, in *Principles and Methods of Toxicology*, 3rd ed (Hayes AW ed) pp 1269, Raven Press Ltd., New York.
- Hakkola J, Raunio H, Purkunen R, Pelkonen O, Saarikoski S, Cresteil T, and Pasanen M (1996) Detection of cytochrome P450 gene expression in human placenta in first trimester of pregnancy. *Biochem Pharmacol* **52**:379–383.
- IARC Working Group on the Evaluation of Carcinogenic Risks to Humans (2002) Some traditional herbal medicines, some mycotoxins, naphthalene and styrene. *IARC Monogr Eval Carcinog Risks Hum* **82**:1–556.
- Ingelman-Sundberg M (2002) Polymorphism of cytochrome P450 and xenobiotic toxicity. *Toxicology* **181–182**:447–452.
- Kitagawa K, Kunugita N, Kitagawa M, and Kawamoto T (2001) CYP2A6*6, a novel polymorphism in cytochrome P450 2A6, has a single amino acid substitution (R128Q) that inactivates enzymatic activity. *J Biol Chem* **276**:17830–17835.
- Lanza DL, Code E, Crespi CL, Gonzalez FJ, and Yost GS (1999) Specific dehydrogenation of 3-methylindole and epoxidation of naphthalene by recombinant human CYP2F1 expressed in lymphoblastoid cells. *Drug Metab Dispos* **27**:798–803.
- Lorenz J, Glatt HR, Fleischmann R, Ferlinz R, and Oesch F (1984) Drug metabolism in man and its relationship to that in three rodent species: monooxygenase, epoxide hydrolase and glutathione S-transferase activities in subcellular fractions of lung and liver. *Biochem Med* **32**:43–56.
- Nagata K, Martin BM, Gillette JR, and Sasame HA (1990) Isozymes of cytochrome P-450 that metabolize naphthalene in liver and lung of untreated mice. *Drug Metab Dispos* **18**:557–564.
- National Toxicology Program (1992) Toxicology and carcinogenesis studies of naphthalene (CAS no. 91-20-3) in B6C3F1 mice (inhalation studies). *Natl Toxicol Program Tech Rep Ser* **410**:1–172.
- National Toxicology Program (2000) Toxicology and carcinogenesis studies of naphthalene (CAS no. 91-20-3) in F344/N rats (inhalation studies). *Natl Toxicol Program Tech Rep Ser* **500**:1–173.
- Nichols WK, Mehta R, Skordos K, Mace K, Pfeifer AM, Carr BA, Minko T, Burchiel SW, and Yost GS (2003) 3-Methylindole-induced toxicity to human bronchial epithelial cell lines. *Toxicol Sci* **71**:229–236.
- Nishimura M, Yaguti H, Yoshitsugu H, Naito S, and Satoh T (2003) Tissue distribution of mRNA expression of human cytochrome P450 isoforms assessed by high-sensitivity real-time reverse transcription PCR. *Yakugaku Zasshi* **123**:369–375.
- Omura T and Sato R (1964) The carbon monoxide binding pigment of liver microsomes. I. Evidence for its hemoprotein nature. *J Biol Chem* **239**:2370–2378.
- Pacifici GM, Boobis AR, Brodie MJ, McManus ME, and Davies DS (1981) Tissue and species differences in enzymes of epoxide metabolism. *Xenobiotica* **11**:73–79.
- Plopper CG, Suverkropp C, Morin D, Nishio S, and Buckpitt A (1992) Relationship of cytochrome P-450 activity to Clara cell cytotoxicity. I. Histopathologic comparison of the respiratory tract of mice, rats and hamsters after parenteral administration of naphthalene. *J Pharmacol Exp Ther* **261**:353–363.
- Rasmussen RE, Do DH, Kim TS, and Dearden LC (1986) Comparative cytotoxicity of naphthalene and its monomethyl- and mononitro-derivatives in the mouse lung. *J Appl Toxicol* **6**:13–20.
- Ritter JK, Owens IS, Negishi M, Nagata K, Sheen YY, Gillette JR, and Sasame HA (1991) Mouse pulmonary cytochrome P-450 naphthalene hydroxylase: cDNA cloning, sequence and expression in *Saccharomyces cerevisiae*. *Biochemistry* **30**:11430–11437.
- Sauer JM, Eversole RR, Lehmann CL, Johnson DE, and Beuving LJ (1997) An ultrastructural evaluation of acute 1-nitronaphthalene induced hepatic and pulmonary toxicity in the rat. *Toxicol Lett (Shannon)* **90**:19–27.
- Sheets PL, Yost GS, and Carlson GP (2004) Benzene metabolism in human lung cell lines BEAS-2B and A549 and cells overexpressing CYP2F1. *J Biochem Mol Toxicol* **18**:92–99.
- Shultz MA, Choudary PV, and Buckpitt AR (1999) Role of murine cytochrome P-450 2F2 in metabolic activation of naphthalene and metabolism of other xenobiotics. *J Pharmacol Exp Ther* **290**:281–288.
- Shultz MA, Morin D, Chang AM, and Buckpitt A (2001) Metabolic capabilities of CYP2F2 with various pulmonary toxicants and its relative abundance in mouse lung subcompartments. *J Pharmacol Exp Ther* **296**:510–519.
- Simmonds AC, Reilly CA, Baldwin RM, Ghanayem BI, Lanza DL, Yost GS, Collins KS, and Forkert PG (2004) Bioactivation of 1,1-dichloroethylene to its epoxide by CYP2E1 and CYP2F enzymes. *Drug Metab Dispos* **32**:1032–1039.
- Simons PC and Vander Jagt DL (1981) Purification of glutathione S-transferases by glutathione-affinity chromatography. *Methods Enzymol* **77**:235–237.
- Strobel HW and Dignam JD (1978) Purification and properties of NADPH-cytochrome P-450 reductase. *Methods Enzymol* **52**:89–96.
- Thornton-Manning J, Appleton ML, Gonzalez FJ, and Yost GS (1996) Metabolism of 3-methylindole by vaccinia-expressed P450 enzymes: correlation of 3-methyleneindolenine formation and protein-binding. *J Pharmacol Exp Ther* **276**:21–29.
- Verschoye RD, Carthew P, Wolf CR, and Dinsdale D (1993) 1-Nitronaphthalene toxicity in rat lung and liver: effects of inhibiting and inducing cytochrome P450 activity. *Toxicol Appl Pharmacol* **122**:208–213.
- Wang H, Lanza DL, and Yost GS (1998) Cloning and expression of CYP2F3, a cytochrome P450 that bioactivates the selective pneumotoxins 3-methylindole and naphthalene. *Arch Biochem Biophys* **349**:329–340.
- Warren DL, Brown DL Jr, and Buckpitt AR (1982) Evidence for cytochrome P-450 mediated metabolism in the bronchiolar damage by naphthalene. *Chem-Biol Interact* **40**:287–303.
- Watt KC and Buckpitt AR (2000) Species differences in the regio- and stereoselectivity of 1-nitronaphthalene metabolism. *Drug Metab Dispos* **28**:376–378.
- Watt KC, Morin DM, Kurth MJ, Mercer RS, Plopper CG, and Buckpitt AR (1999) Glutathione conjugation of electrophilic metabolites of 1-nitronaphthalene in rat tracheobronchial airways and liver: identification by mass spectrometry and proton nuclear magnetic resonance spectroscopy. *Chem Res Toxicol* **12**:831–839.
- West JA, Pakeham G, Morin D, Fleschner CA, Buckpitt AR, and Plopper CG (2001) Inhaled naphthalene causes dose dependent Clara cell cytotoxicity in mice but not in rats. *Toxicol Appl Pharmacol* **173**:114–119.
- Yamano S, Tatsuno J, and Gonzalez FJ (1990) The CYP2A3 gene product catalyzes coumarin 7-hydroxylation in human liver microsomes. *Biochemistry* **29**:1322–1329.

Address correspondence to: R. Michael Baldwin, Veterinary Medicine: Molecular Biosciences, 1311 Haring Hall, UC Davis, Davis, CA 95616. E-mail: rmbaldwin@ucdavis-alumni.com
